



SIMULATION OPTIMIZATION SYSTEMS
Research Laboratory

**AUTOMATED EM OPTIMIZATION OF
LINEAR AND NONLINEAR CIRCUITS
WITH GEOMETRY CAPTURE
FOR ARBITRARY PLANAR STRUCTURES**

J.W. Bandler, R.M. Biernacki, Q. Cai,
S.H. Chen and P.A. Grobelny

SOS-95-4-R

February 1995



**AUTOMATED EM OPTIMIZATION OF
LINEAR AND NONLINEAR CIRCUITS
WITH GEOMETRY CAPTURE
FOR ARBITRARY PLANAR STRUCTURES**

**J.W. Bandler, R.M. Biernacki, Q. Cai,
S.H. Chen and P.A. Grobelny**

SOS-95-4-R

February 1995

© J.W. Bandler, R.M. Biernacki, Q. Cai, S.H. Chen and P.A. Grobelny 1995

No part of this document may be copied, translated, transcribed or entered in any form into any machine without written permission. Address enquiries in this regard to Dr. J.W. Bandler. Excerpts may be quoted for scholarly purposes with full acknowledgement of source. This document may not be lent or circulated without this title page and its original cover.

AUTOMATED EM OPTIMIZATION OF LINEAR AND NONLINEAR CIRCUITS WITH GEOMETRY CAPTURE FOR ARBITRARY PLANAR STRUCTURES

John W. Bandler, *Fellow, IEEE*, Radoslaw M. Biernacki, *Senior Member, IEEE*,
Qian Cai, *Member, IEEE*, Shao Hua Chen, *Member, IEEE*, and Piotr A. Grobelny

Abstract

This paper presents a ground-breaking approach to integrating previously disjoint simulation technologies for automated electromagnetic (EM) optimization of linear and nonlinear microwave circuits. We seamlessly integrate EM analyses with harmonic balance optimization of nonlinear circuits. We also pioneer statistical circuit optimization simultaneously incorporating SPICE models of active devices and EM models of passive microstrip structures. We introduce an exciting breakthrough: our Geometry Capture technique which makes EM optimization of arbitrary planar structures a reality. Designable parameters are captured graphically from the layout and the layout is directly optimized without the need of any schematic translation. Design of a comprehensive class B frequency doubler and a broad-band small-signal amplifier demonstrate our approach.

This work was supported in part by Optimization Systems Associates Inc. and in part by the Natural Sciences and Engineering Research Council of Canada under Grants OGP0007239, OGP0042444 and STR0167080. Additional support was provided through a Natural Sciences and Engineering Research Council of Canada Industrial Research Fellowship granted to Q. Cai.

J.W. Bandler, R.M. Biernacki and S.H. Chen are with Optimization Systems Associates Inc., P.O. Box 8083, Dundas, Ontario, Canada L9H 5E7, and the Simulation Optimization Systems Research Laboratory and Department of Electrical and Computer Engineering, McMaster University, Hamilton, Ontario, Canada L8S 4L7.

Q. Cai is with Optimization Systems Associates Inc., P.O. Box 8083, Dundas, Ontario, Canada L9H 5E7.

P.A. Grobelny is with the Simulation Optimization Systems Research Laboratory and Department of Electrical and Computer Engineering, McMaster University, Hamilton, Ontario, Canada L8S 4L7.

I. INTRODUCTION

Electromagnetic (EM) simulators cannot realize their full potential in circuit design unless they are embedded into circuit- and system-level simulation environments and driven by automated optimization algorithms [1]. Without such an integration, EM simulators can only be used to validate designs obtained from optimizing equivalent or empirical circuit models, or to generate look-up tables outside the optimization loop. If the optimized equivalent or empirical circuit model is invalidated, the designer may have to resort to manual adjustments involving repeated EM simulations in a tedious process.

Our pioneering work in interfacing EM simulators with circuit optimizers has captivated the attention of leading researchers and designers, already generating many exciting developments [2-6]. We refined interpolation and modeling techniques [2, 3, 7-9] in order to reconcile the discrete nature of numerical EM solvers and the requirement of the optimizers for continuous variables and gradients. We introduced an integrated data base system to store the simulation results of EM analyses. However, our initial efforts were confined to a library of predefined elementary structures such as microstrip lines, steps and T -junctions. Complicated structures had to be decomposed into elements in the library, individually simulated, and the EM results are then connected in a circuit-theoretic fashion [2, 3]. The primary disadvantage of that approach is that possible couplings between different elements are not taken into account.

In this paper, we present a ground-breaking approach to integrating previously disjoint simulation technologies for automated EM optimization of linear and nonlinear microwave circuits. We introduce an exciting breakthrough: our Geometry Capture technique which makes EM optimization of arbitrary planar structures a reality [10]. Designable parameters are captured graphically from the layout and the layout is directly optimized without the need of any schematic translation. Furthermore, designable parameters are not limited to geometrical dimensions, but can also include substrate and metallization parameters.

For nonlinear circuits, we seamlessly integrate EM analyses with harmonic balance (HB) optimization. For circuits containing active devices, we take advantage of the accurate EM models

for passive components and the popular and time-tested SPICE models for active devices. The process of invoking the two independent types of simulations and combining the results at the circuit level is automated to facilitate both nominal and statistical designs. Our work lays the software architectural foundation for a new generation of CAD systems with emphasis on the integration of heterogenous tools.

Our approach is implemented within the friendly optimization environment OSA90/hope [7] featuring a circuit-level HB simulator, connecting to the EM simulator *em* from Sonnet Software [11] through Empipe [12], and connecting to SPICE [13] through Spicepipe [14]. The flexibility and benefits of our approach are illustrated by the design of two microwave circuits. The novel combination of EM simulation and HB optimization is demonstrated by a comprehensive class B frequency doubler design. Nominal and statistical designs of a broad-band small-signal amplifier containing microstrip components exemplify the utilization of SPICE device models together with EM simulations.

II. INTEGRATION OF EM AND HB SIMULATION

Large-signal circuit optimization with the HB technique has been significantly advanced during the last decade (e.g., [15-19]). The computational time has been greatly reduced due to the efficiency of the HB simulation and an elegant sensitivity calculation [17]. HB optimization using the FAST sensitivity technique has been applied to performance- and yield-driven designs [18, 19].

In general, a nonlinear circuit can be partitioned into a nonlinear subcircuit, a linear subcircuit and an excitation subcircuit as shown in Fig. 1. The linear subcircuit can be further divided into a lumped element subcircuit and a microstrip element subcircuit also shown in Fig.

1. Let the circuit parameters be

$$\phi = \left[\phi_N^T \quad \phi_{LL}^T \quad \phi_{LM}^T \right]^T \quad (1)$$

where ϕ_N are the parameters of the nonlinear subcircuit, ϕ_{LL} and ϕ_{LM} are the parameters of the lumped element subcircuit and the microstrip element subcircuit, respectively. The HB equation of the circuit can be written as

$$\mathbf{F}(\phi, \mathbf{V}(\phi)) = \mathbf{I}(\phi, \mathbf{V}(\phi)) + j\Omega\mathbf{Q}(\phi, \mathbf{V}(\phi)) + \mathbf{Y}(\phi)\mathbf{V}(\phi) + \mathbf{I}_s = \mathbf{0} \quad (2)$$

where \mathbf{V} is the vector of nonlinear port voltages to be solved for, \mathbf{I} and \mathbf{Q} the vectors of currents and charges entering the nonlinear ports, respectively, Ω the angular frequency matrix, \mathbf{I}_s the vector of equivalent excitation currents, and \mathbf{Y} the equivalent admittance matrix of the linear subcircuit corresponding to the connection ports. \mathbf{Y} is a function of frequency f and parameters of the linear subcircuit ϕ_{LL} and ϕ_{LM} , which can be expressed as

$$\mathbf{Y}(\phi) = \mathbf{Y}(f, \phi_{LL}, \mathbf{R}_{EM}(f, \phi_{LM})) \quad (3)$$

where $\mathbf{R}_{EM}(f, \phi_{LM})$ represents the EM responses.

Once $\mathbf{R}_{EM}(f, \phi_{LM})$ is returned from the EM simulator $\mathbf{Y}(\phi)$ is obtained from (3) and then the HB equation (2) is solved. The Newton update for solving (2) can be written as

$$\mathbf{V}_{new}(\phi) = \mathbf{V}_{old}(\phi) - [\mathbf{J}(\phi, \mathbf{V}_{old}(\phi))]^{-1}\mathbf{F}(\phi, \mathbf{V}_{old}(\phi)) \quad (4)$$

where $\mathbf{J}(\phi, \mathbf{V}(\phi))$ is the Jacobian matrix.

III. GRADIENT-BASED DIRECT HB AND EM OPTIMIZATION

Consider a vector of circuit responses

$$\mathbf{R}_{CT}(\phi) = \mathbf{R}(\phi, \mathbf{V}(\phi, \mathbf{R}_{EM}(\phi))) \quad (5)$$

which may include output voltages, currents, powers, power gains, etc. From these responses and the corresponding design specifications, we can formulate an appropriate objective function, such as minimax, ℓ_1 , ℓ_2 or Huber function, for optimization. For gradient-based optimization we need

to calculate the derivatives of the circuit responses R_{CT} w.r.t. each design variable ϕ_i in ϕ . $\partial R_{CT}/\partial \phi_i$ can be derived from (5) as

$$\frac{\partial R_{CT}}{\partial \phi_i} = \frac{\partial R}{\partial \phi_i} + \left[\frac{\partial R^T}{\partial V} \right]^T \left(\frac{\partial V}{\partial \phi_i} + \left[\frac{\partial V^T}{\partial R_{EM}} \right]^T \frac{\partial R_{EM}}{\partial \phi_i} \right) \quad (6)$$

which can be evaluated using an elegant gradient estimation technique [3].

The complete design optimization process is illustrated by the flowchart shown in Fig. 2.

IV. GEOMETRY CAPTURE FOR EM OPTIMIZATION OF ARBITRARY STRUCTURES

One of the most attractive advantages of EM simulators is the ability to analyze structures of arbitrary geometry. Naturally, EM simulator users wish to be able to designate optimizable parameters directly within the graphical layout representation. To satisfy their wish, we must be able to relate geometrical coordinates of the layout to the numerical parameters for optimization. To automate such a parameterization process is quite a challenge.

An Empire element library [2, 3, 12] was created in our earlier work. The library contains geometrical primitives (lines, bends, junctions, gaps, stubs, etc.) from which a subcircuit structure can be built. This approach gained immediate acceptance by CAD users by virtue of its familiarity and ease of use. Also, it minimizes the complexity of EM analysis since each time only one elementary geometry is analyzed. However, this approach inherently omits possible proximity couplings between the elements since they are connected by the circuit-level simulator. Furthermore, it does not accommodate structures which cannot be decomposed into library elements.

To provide a tool for parameterizing arbitrary structures we created the user-friendly "Geometry Capture" tool [10]. Geometry Capture facilitates automatic translation of the values of user-defined designable parameters to the layout description in terms of absolute coordinates (the latter is the required input to EM simulators). During optimization, this translation is automatically performed for each new set of parameter values before the EM simulator is invoked.

Using a graphical layout editing tool (such as *xgeom* for *em* from Sonnet Software [11]), the user generates a set of geometries marking the evolution of the structure under consideration as the designable parameters change. For example, consider parameterization of the simple step structure shown in Fig. 3. Two parameters, the width W and length L , are selected as designable. The evolution of the structure is described by the nominal structure, the structure reflecting a change in W and the structure reflecting a change in L . The Geometry Capture form editor with the corresponding data entries is shown in Fig. 4. The first three entries are names of the files containing the nominal geometry, the control parameters and the optional DC S -parameter data, respectively. The following two entries refer to the geometries generated with perturbed values of W and L . The resulting information is then processed by Empipe to establish the mapping between the designable parameter values and the geometrical coordinates.

V. EM/HB OPTIMIZATION INTEGRATED WITH SPICE DEVICE MODELING

A. Capturing SPICE Device Models

The public domain SPICE program does not provide any means for optimization. Incorporating the results of EM simulations of passive subcircuits into SPICE requires an equivalent circuit representation and is not available in an automated fashion for optimization. The rigid structure of commercial versions of SPICE permits only limited optimization.

SPICE device models are highly regarded by the microwave community. In our work SPICE is interconnected to OSA90/hope through the Spicepipe interface [14]. The interface allows for OSA90/hope to drive SPICE in an automated manner, with the SPICE input data determined in OSA90/hope and the SPICE results returned to OSA90/hope.

SPICE is invoked to simulate the device only. The SPICE output is returned to OSA90/hope and postprocessed. This is achieved using the expression processing capabilities of OSA90/hope, for example simulated node voltages are converted to the S parameters of the device. In fact, two SPICE simulations are carried out to determine the parameters of a 2-port network.

Assuming that in addition to the nonlinear and the microstrip subcircuits there are m devices in the circuit, all to be simulated by SPICE, the overall circuit responses in (5) can now be expressed as

$$R_{CT}(\phi) = R(\phi, V(\phi), R_{EM}(\phi), R_{SP}^1(\phi), R_{SP}^2(\phi), \dots, R_{SP}^m(\phi)) \quad (7)$$

where $R_{SP}^1(\phi), R_{SP}^2(\phi), \dots, R_{SP}^m(\phi)$ are the SPICE simulated responses of the m device subcircuits.

B. Statistical Parameter Extraction with SPICE and OSA90/hope

Suppose there are n_d sets of data measured from n_d devices and n_i measured responses in the i th data set

$$S^i = [S_1^i \ S_2^i \ \dots \ S_{n_i}^i]^T, \quad i = 1, 2, \dots, n_d \quad (8)$$

Corresponding to S^i we have the SPICE responses

$$R_{SP}(\phi^i) = [R_{SP_1}(\phi^i) \ R_{SP_2}(\phi^i) \ \dots \ R_{SP_{n_i}}(\phi^i)]^T, \quad i = 1, 2, \dots, n_d \quad (9)$$

where ϕ^i is the i th set of model parameters to be extracted.

The error and objective functions are constructed in OSA90/hope. Let the error vector be

$$e_{OS}(\phi^i) = [e_{OS_1}(\phi^i) \ e_{OS_2}(\phi^i) \ \dots \ e_{OS_{n_i}}(\phi^i)]^T \quad (10)$$

where

$$e_{OS_j}(\phi^i) = R_{SP_j}(\phi^i) - S_j^i \quad (11)$$

then the parameter extraction problem can be defined as

$$\underset{\phi^i}{\text{minimize}} \ U_{OS}(\phi^i) \triangleq H[e_{OS}(\phi^i)] \quad (12)$$

where U_{OS} is the objective function created in OSA90/hope and H represents a norm of the error vector such as the ℓ_1 , ℓ_2 or the Huber norm [7]. For each device outcome the parameter extraction is driven by OSA90/hope's optimizer with the SPICE device model captured as described in the previous subsection. The model responses are compared by OSA90/hope against measured data. This leads to a sample of individually extracted device models. The model statistics including the mean values, standard deviations and the correlation matrix are produced by HarPE [20] through postprocessing this sample of models.

C. Automated Optimization Environment

Fig. 5 depicts the optimization environment incorporating the *em* simulator and SPICE device models. In this environment Geometry Capture for arbitrary microstrip structures complements the Empipe library of typical primitives. In our implementation the Empipe and Spicepipe interfaces between OSA90/hope and *em* and SPICE are based on the Datapipe technology [7, 21]. The Datapipe technology is an open software architecture developed to create and maintain efficient connections between several independent CAD tools. A review of the Datapipe technology is given in the Appendix.

VI. SIMULATION AND OPTIMIZATION OF A CLASS B FREQUENCY DOUBLER

A class B frequency doubler is used as an example to demonstrate our new approach of integrated HB/EM simulation and optimization. The circuit structure, shown in Fig. 6, follows [22]. It consists of a single FET (NE71000) and a number of distributed microstrip elements including two radial stubs and two large bias pads.

Significant couplings between the distributed microstrip elements exist in this circuit, e.g., the couplings between the radial stubs and the bias pads. The conventional approach using empirical or physical models for individual microstrip elements neglects these couplings and therefore may result in large response errors. In order to take into account these couplings the entire microstrip structure should be considered as a single element to be simulated and optimized.

The design specifications are

$$\text{conversion gain} \geq 3 \text{ dB}$$

$$\text{spectral purity} \geq 20 \text{ dB}$$

at 7 GHz and 10 dBm input power.

We use the Curtice and Ettenberg FET model [23] to model the FET NE71000. The model parameters are extracted from the typical DC and S parameters [24] using HarPE [20].

The entire microstrip structure between the two capacitors (see Fig. 6) is parameterized using our Geometry Capture and considered as one element to be simulated by *em*. The results are directly returned to OSA90/hope through Empipe for HB simulation and optimization. Ten parameters denoted as P_1, P_2, \dots, P_{10} are selected as design variables. The Geometry Capture form editor for this structure is shown in Fig. 7. Notice, that the HB analysis requires the DC S parameters to be specified. The minimax optimizer of OSA90/hope directs the performance-driven design.

The values of the design variables before and after optimization are listed in Table I. The conversion gain versus input power before and after optimization is shown in Fig. 8. The source and output voltage waveforms before and after optimization are plotted in Fig. 9. The 3D view of conversion gain versus frequency and input power before and after optimization are shown in Fig. 10. Significant improvement of the circuit performance is obtained and all specifications are satisfied after optimization.

VII. NOMINAL AND STATISTICAL DESIGN OF A SMALL-SIGNAL AMPLIFIER

To illustrate design utilizing simultaneously EM simulations and SPICE device modeling we consider a broadband small-signal amplifier with microstrip components [2] as shown in Fig. 11. The specification is

$$7 \text{ dB} \leq |S_{21}| \leq 8 \text{ dB} \quad \text{for} \quad 6 \text{ GHz} \leq f \leq 18 \text{ GHz}$$

where f is the frequency. The microstrip components are accurately simulated by *em* utilizing the line and the T -structure primitives of the Empipe [12] library. The MESFET is simulated by SPICE using the model shown in Fig. 12. There are 18 model parameters. The parameter statistics have been extracted from the synthetic data generated by Monte Carlo simulation using the model given in [2] and include the mean values, standard deviations, discrete density functions (DDF) and correlation matrix. The parameter mean values and standard deviations are listed in Table II. The circuit-level simulation and optimization are carried out by OSA90/hope.

Each of the microstrip T -structures is defined by six geometrical parameters and the feedback microstrip line is defined by two geometrical parameters, see Fig. 13. Following [2], we choose $W_{g1}, L_{g1}, W_{g2}, L_{g2}$ of the gate T -structure and $W_{d1}, L_{d1}, W_{d2}, L_{d2}$ of the drain T -structure as design variables. W_{g3}, L_{g3}, W_{d3} and L_{d3} of the T -structures, W and L of the feedback microstrip line, as well as the MESFET parameters are not optimized. The small-signal gain before and after optimization in nominal design are plotted in Fig. 14.

For statistical design we assume a uniform distribution with 0.5 mil tolerance for all geometrical parameters. Yield at the nominal minimax solution is 43%. It is increased to 74% after yield optimization, which was performed using 50 outcomes. Fig. 15 shows the run charts before and after yield optimization for all of the 250 outcomes used in yield estimations at the frequency of 18 GHz. Clearly, many more outcomes meet the specification on $|S_{21}|$ after yield optimization. Table III lists values of the geometrical parameters at the nominal minimax solution and at the centered design.

VIII. CONCLUSIONS

We have presented an integrated approach to EM optimization of linear and nonlinear microwave and millimeter-wave circuits. Our Geometry Capture technique has removed barriers which previously confined EM optimization to a limited number of predefined elements. This has broadened the horizon of exciting applications for microwave engineers to accurately design circuits consisting of complicated structures and investigate new microstrip components. For the first time,

we have integrated EM simulations directly with nonlinear HB simulation and optimization. Moreover, we have combined accurate EM models of passive microstrip structures with SPICE device models for nominal and statistical optimization. Our new approach has been demonstrated through the optimization of a class B frequency doubler as well as the nominal and statistical designs of a broad-band small-signal amplifier. Our approach can be extended to the integration of physical and physics-based device simulators.

IX. ACKNOWLEDGEMENT

The authors thank Dr. J.C. Rautio, President of Sonnet Software, Inc., Liverpool, NY, for making *em* and *xgeom* available for this work.

X. APPENDIX

Our intelligent optimization interface is based on the Datapipe technique [7, 21]. Datapipes utilize UNIX's interprocess pipe communication facility to establish high speed data connections between cooperating processes.

In UNIX a pipe is an I/O channel intended for use between two interacting processes. One process writes into the pipe, while the other process reads from the pipe. UNIX, as the operating system, controls buffering of the data and synchronization of the two processes. The system call `pipe()` creates a pipe and returns two file descriptors, one for the read side and the other one for the write side of the pipe. These descriptors, being file identifiers, may be used in `read()`, `write()` and `close()` calls just like a typical disk file descriptor. If a process reads from a pipe which is empty, it waits until data arrives; if a process writes into a pipe which is full, it waits until the pipe is emptied somehow. Once the pipes have been created by the call to `pipe()` the process uses the `fork()` system call to create a copy of itself. Then, the child copy of the process, calls the system shell to execute the desired child program.

A schematic of the Datapipe interface between a parent process and a number of child processes is shown in Fig. 16. The parent communicates with each child through a Datapipe

protocol at the parent side and a Datapipe server at the child side. The Datapipe protocol consisting of a set of communication standards defines the sequence and meaning of the data fields to be exchanged between the parent and the child. The Datapipe server is a set of functions to be included in the child for reading data from and writing data to the parent. The parent and the child can be totally independent. This is especially suitable for sensitive software since the source code does not need to be revealed.

In general, there is no limit to the number of children that can be interconnected with a single parent through Datapipes. Furthermore, the parent and the children can run on different computers connected in a network. This facilitates parallel processing, which can significantly speed up CPU intensive optimization [25].

In the context of this paper (Fig. 5) the OSA90/hope optimization system is the parent program and the Empipe and Spicepipe interfaces to *em* and SPICE are sophisticated child programs. It is clear that other simulators could be interfaced to OSA90/hope in a similar manner.

XI. REFERENCES

- [1] J.W. Bandler, "Circuit design with direct optimization-driven electromagnetic simulators," *IEEE MTT-S Int. Microwave Symposium, Panel Session on Circuit Design with Direct Optimization-Driven Electromagnetic Simulators* (San Diego, CA), 1994.
- [2] J.W. Bandler, R.M. Biernacki, S.H. Chen, P.A. Grobelny and S. Ye, "Yield-driven electromagnetic optimization via multilevel multidimensional models," *IEEE Trans. Microwave Theory Tech.*, vol. 41, 1993, pp. 2269-2278.
- [3] J.W. Bandler, R.M. Biernacki, S.H. Chen, D.G. Swanson, Jr., and S. Ye, "Microstrip filter design using direct EM field simulation," *IEEE Trans. Microwave Theory Tech.*, vol. 42, 1994, pp. 1353-1359.
- [4] J.W. Bandler, R.M. Biernacki, S.H. Chen and P.A. Grobelny, "A CAD environment for performance and yield driven circuit design employing electromagnetic field simulators," *Proc. Int. Symp. Circuits and Systems* (London, England), vol. 1, 1994, pp. 145-148.
- [5] P.P.M. So, W.J.R. Hofer, J.W. Bandler, R.M. Biernacki and S.H. Chen, "Hybrid frequency/time domain field theory based CAD of microwave circuit," *Proc. 23rd European Microwave Conf.* (Madrid, Spain), 1993, pp. 218-219.
- [6] R. Griffith, E. Chiprout, Q.J. Zhang and M. Nakhla, "A CAD framework for simulation and optimization of high-speed VLSI interconnections," *IEEE Trans. Circuits and Systems*, vol. 39, 1992, pp. 893-906.

- [7] *OSA90/hope*[™], Optimization Systems Associates Inc., P.O. Box 8083, Dundas, Ontario, Canada L9H 5E7, 1994.
- [8] R.M. Biernacki and M.A. Styblinski, "Efficient performance function interpolation scheme and its application to statistical circuit design," *IEEE Int. J. Circuit Theory and Appl.*, vol. 19, 1991, pp. 403-422.
- [9] R.M. Biernacki, J.W. Bandler, J. Song and Q.J. Zhang, "Efficient quadratic approximation for statistical design," *IEEE Trans. Circuits and Systems*, vol. 36, 1989, pp. 1449-1454.
- [10] J.W. Bandler, R.M. Biernacki, Q. Cai, S.H. Chen and P.A. Grobelny, "Integrated harmonic balance and electromagnetic optimization with Geometry Capture," *IEEE MTT-S Int. Microwave Symp.* (Orlando, FL), 1995.
- [11] *em*[™] and *xgeom*[™], Sonnet Software, Inc., Suite 203, 135 Old Cove Road, Liverpool, NY 13090-3774, 1994.
- [12] *Empipe*[™], Optimization Systems Associates Inc., P.O. Box 8083, Dundas, Ontario, Canada L9H 5E7, 1994.
- [13] T. Quarles, A.R. Newton, D.O. Pederson and A. Sangiovanni-Vincentelli, *SPICE3 Version 3f4 User's Manual*. Department of Electrical Engineering and Computer Sciences, University of California, Berkeley, CA, 1993.
- [14] *Spicepipe*[™], Optimization Systems Associates Inc., P.O. Box 8083, Dundas, Ontario, Canada L9H 5E7, 1994.
- [15] V. Rizzoli, A. Lipparini and E. Marazzi, "A general-purpose program for nonlinear microwave circuit design," *IEEE Trans. Microwave Theory Tech.*, vol. 31, 1983, pp. 762-770.
- [16] K.S. Kundert and A. Sangiovanni-Vincentelli, "Simulation of nonlinear circuits in the frequency domain," *IEEE Trans. Computer-Aided Design*, vol. CAD-5, 1986, pp. 521-535.
- [17] J.W. Bandler, Q.J. Zhang and R.M. Biernacki, "A unified theory for frequency domain simulation and sensitivity analysis of linear and nonlinear circuits," *IEEE Trans. Microwave Theory Tech.*, vol. 36, 1988, pp. 1661-1669.
- [18] J.W. Bandler, Q.J. Zhang, J. Song and R.M. Biernacki, "FAST gradient based yield optimization of nonlinear circuits," *IEEE Trans. Microwave Theory Tech.*, vol. 38, 1990, pp. 1701-1710.
- [19] J.W. Bandler, R.M. Biernacki, Q. Cai, S.H. Chen, S. Ye and Q.J. Zhang, "Integrated physics-oriented statistical modeling, simulation and optimization," *IEEE Trans. Microwave Theory Tech.*, vol. 40, 1992, pp. 1374-1400.
- [20] *HarPE*[™], Optimization Systems Associates Inc., P.O. Box 8083, Dundas, Ontario, Canada L9H 5E7, 1994.
- [21] J.W. Bandler, R.M. Biernacki and S.H. Chen, "Design optimization with external simulators," *COMPUMAG 8th Conf. on the Computation of Electromagnetic Fields* (Sorrento, Italy), 1991, pp. 1061-1064.

- [22] "CAD review: the 7GHz doubler circuit," *Microwave Engineering Europe*, May 1994, pp. 43-53.
- [23] W.R. Curtice and M. Ettenberg, "A nonlinear GaAs FET model for use in the design of output circuits for power amplifiers," *IEEE Trans. Microwave Theory Tech.*, vol. MTT-33, 1985, pp. 1383-1394.
- [24] "RF and Microwave Semiconductors," *NEC Data Book*, NEC California Eastern Laboratories, 1994.
- [25] J.W. Bandler, R.M. Biernacki, Q. Cai, S.H. Chen, P.A. Grobelny and D.G. Swanson Jr., "Heterogeneous parallel yield-driven electromagnetic CAD," *IEEE MTT-S Int. Microwave Symp.* (Orlando, FL), 1995.

TABLE I
 FREQUENCY DOUBLER:
 DESIGN VARIABLE VALUES
 BEFORE AND AFTER MINIMAX OPTIMIZATION

Variable	Before Optimization	After Optimization
P_1	1.5	1.494
P_2	8.1	7.820
P_3	3.3	3.347
P_4	5.7	5.992
P_5	2.4	2.550
P_6	2.4	2.305
P_7	1.8	1.750
P_8	7.8	7.827
P_9	4.2	4.242
P_{10}	2.7	2.622

All dimensions are in mm.

TABLE II
PARAMETER MEAN VALUES AND
STANDARD DEVIATIONS OF
THE STATISTICAL SPICE MESFET MODEL

Parameter	Mean	Standard Deviation (%)
C_{gs} (pF)	0.712	2.76
C_{gd} (pF)	0.032	1.79
λ (1/V)	0.297×10^{-3}	3.77
V_{to} (V)	-4.363	2.31
β (A/V ²)	0.0139	2.37
B (1/V)	2.85×10^{-3}	4.08
α (1/V)	1.916	4.04
R_d (Ω)	0.0692	4.03
R_s (Ω)	7.047	1.52
PB (V)	0.186	4.01
R_g (Ω)	1.988	3.56
G_{ds} (1/ Ω)	4×10^{-3}	2.56
C_{ds} (pF)	0.055	1.59
L_g (nH)	0.0076	3.93
L_d (nH)	0.0127	3.46
L_s (nH)	0.104	3.47
C_{ge} (pF)	0.0819	2.75
C_x (pF)	20.0	-

Parameters C_{gs} through PB are the intrinsic SPICE MESFET parameters [13]. Parameters R_g through C_x are the extrinsic parameters (see Fig. 12). C_x is assumed non-statistical.

TABLE III
 MICROSTRIP PARAMETERS
 FOR THE SMALL-SIGNAL AMPLIFIER

Parameter (mil)	Nominal solution	Centered solution
W_{g1}	15.975	14.688
L_{g1}	33.517	38.316
W_{g2}	7.980	8.265
L_{g2}	26.807	28.244
W_{d1}	4.980	4.882
L_{d1}	6.005	8.436
W_{d2}	2.687	2.051
L_{d2}	14.320	19.015

Only the optimized parameters are listed.

The subscripts g and d denote the parameters of the gate and drain T -structures, respectively (see Figs. 11 and 13).

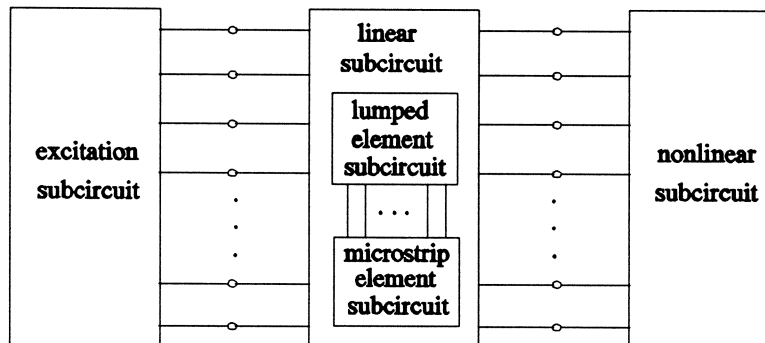


Fig. 1. Partition of a nonlinear microwave circuit for combined HB/EM simulation.

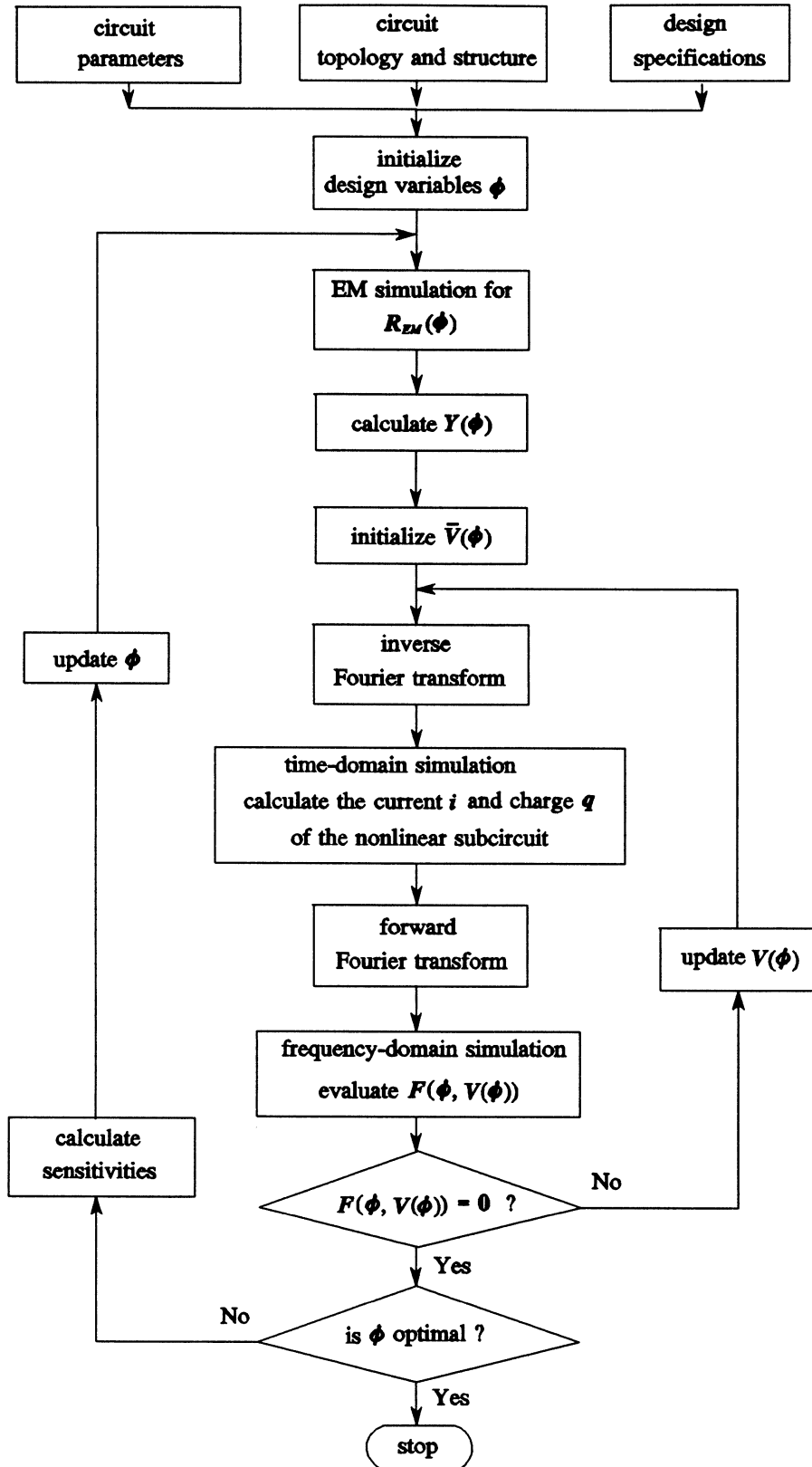


Fig. 2. Flowchart of integrated EM/HB circuit design optimization.

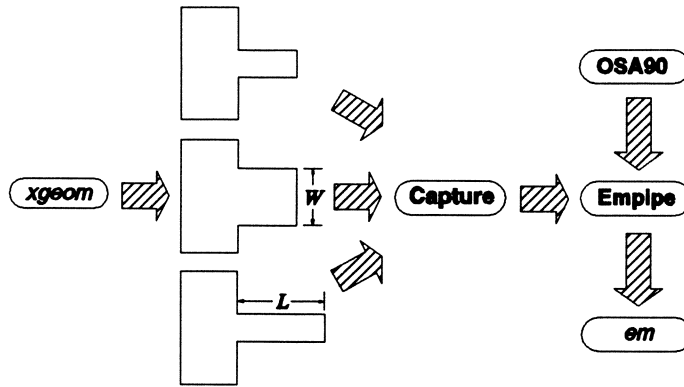


Fig. 3. Illustration of Geometry Capture for parameterizing the step structure w.r.t. L and W .

em parameterization						
Process and Exit			Quit without Processing			
Nominal Geo File:	step.geo					
em Control File:	step.an					
DC S-par File:						
Parameter Name	Geo File Name	Nominal Value	Perturbed Value	# of Grids	Unit Name	
W	step_W.geo	8	16	4	MIL	
L	step_L.geo	16	22	6	MIL	

Fig. 4. Geometry Capture form editor for parameterization of the step structure.

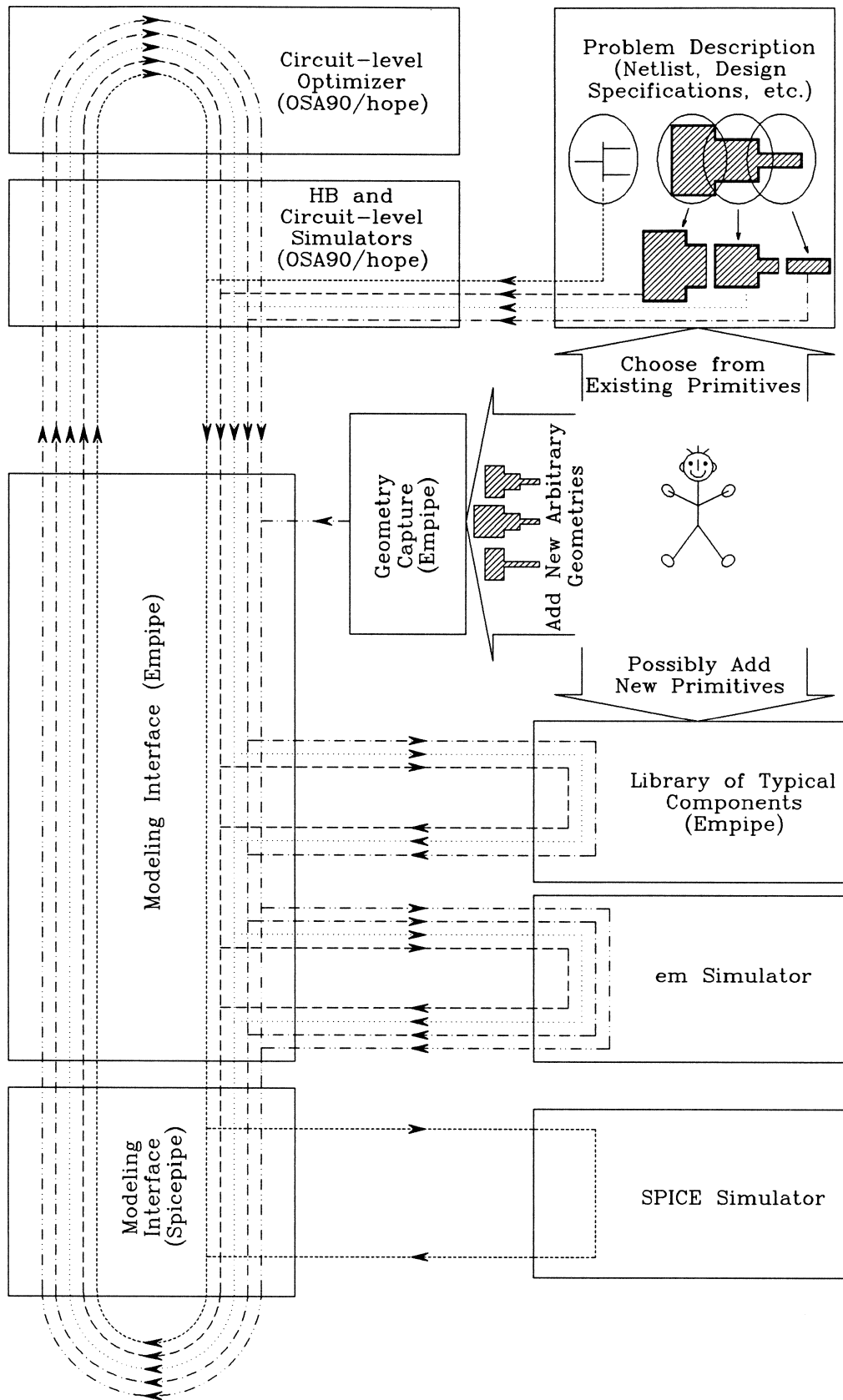


Fig. 5. EM optimization environment combining OSA90/hope's design simulation and optimization with Geometry Capture for arbitrary structures, the Empipe library of typical microstrip primitives and SPICE device modeling.

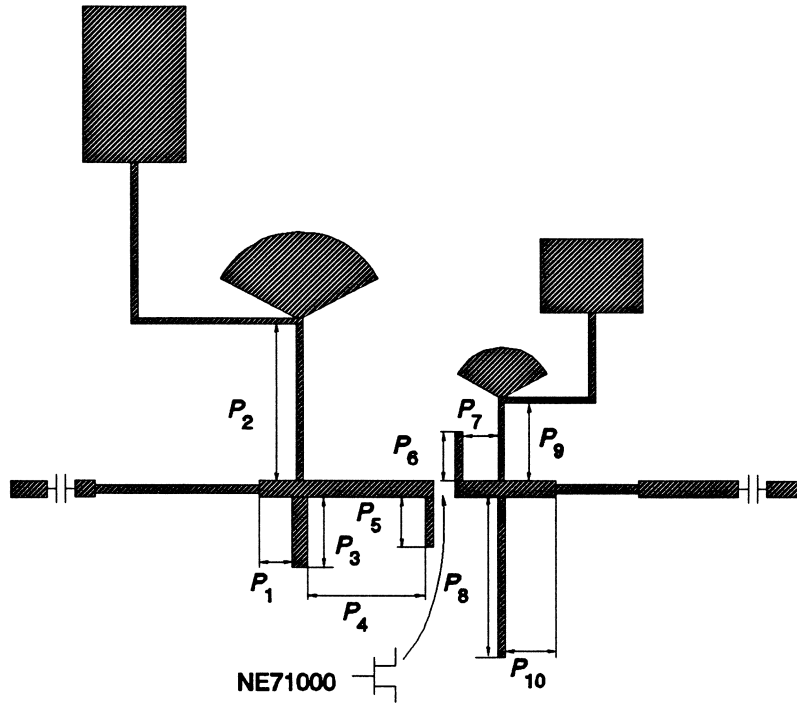


Fig. 6. Circuit structure of the class B frequency doubler.

em parameterization

Nominal Geo File:

em Control File:

DC S-par File:

Parameter Name	Geo File Name	Nominal Value	Perturbed Value	# of Grids	Unit Name
P1	dbl_P1.geo	1.5	1.8	1	MM
P2	dbl_P2.geo	8.1	8.4	1	MM
P3	dbl_P3.geo	3.3	3.6	1	MM
P4	dbl_P4.geo	5.7	6.0	1	MM
P5	dbl_P5.geo	2.4	2.7	1	MM
P6	dbl_P6.geo	2.4	2.7	1	MM
P7	dbl_P7.geo	1.8	2.1	1	MM
P8	dbl_P8.geo	7.8	8.1	1	MM
P9	dbl_P9.geo	4.2	4.5	1	MM
P10	dbl_P10.geo	2.7	3.0	1	MM

Fig. 7. Geometry Capture form editor for parameterization of the microstrip subcircuit of the class B frequency doubler.

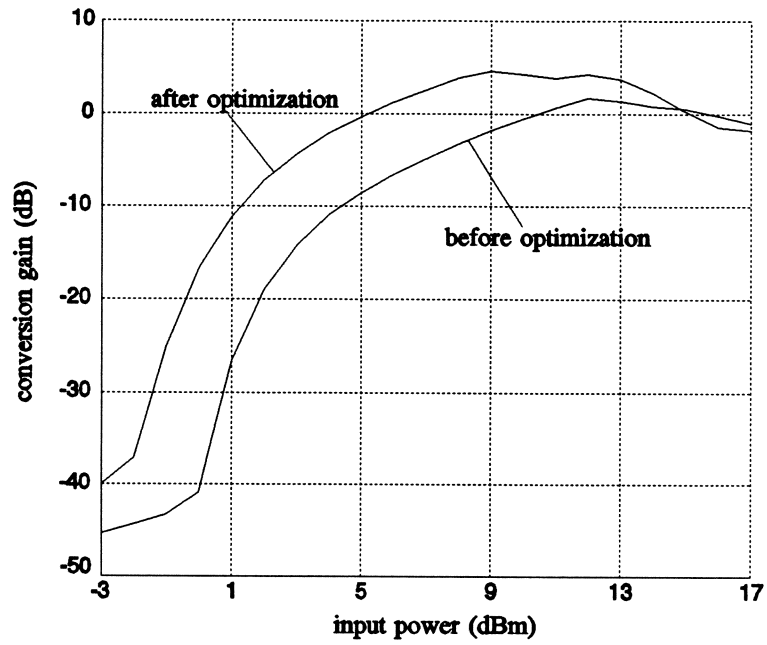


Fig. 8. Conversion gain versus input power before and after optimization.

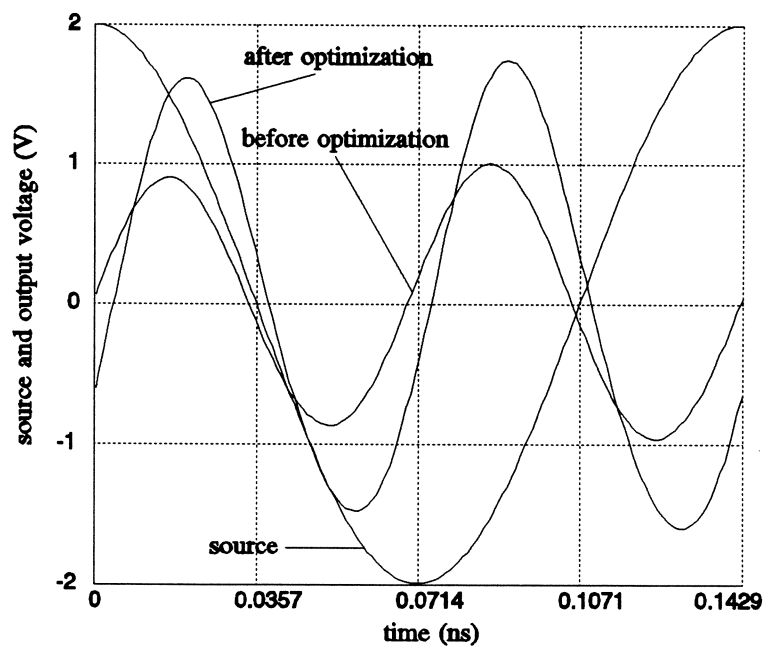


Fig. 9. Source and output voltage waveforms before and after optimization.

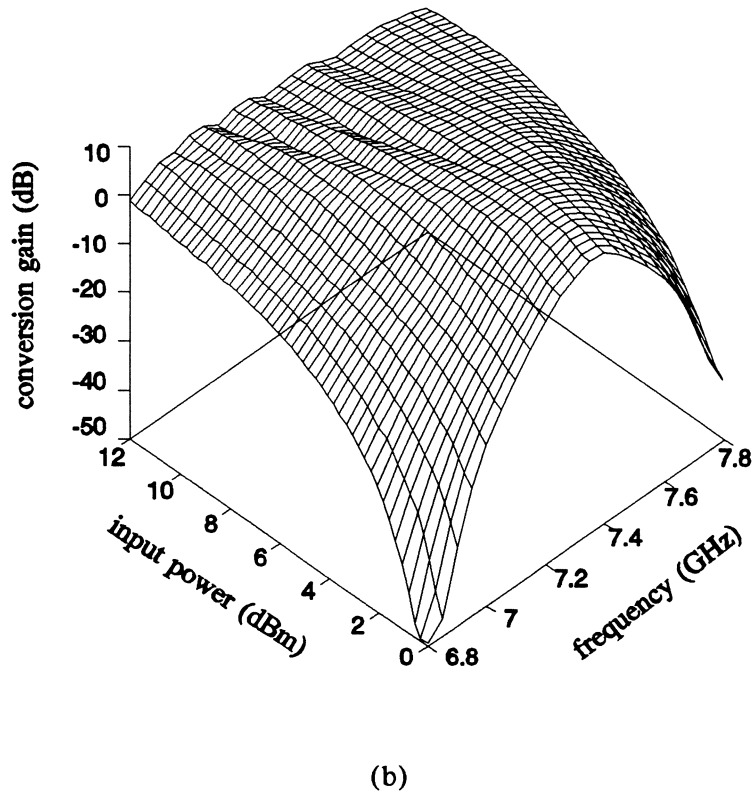
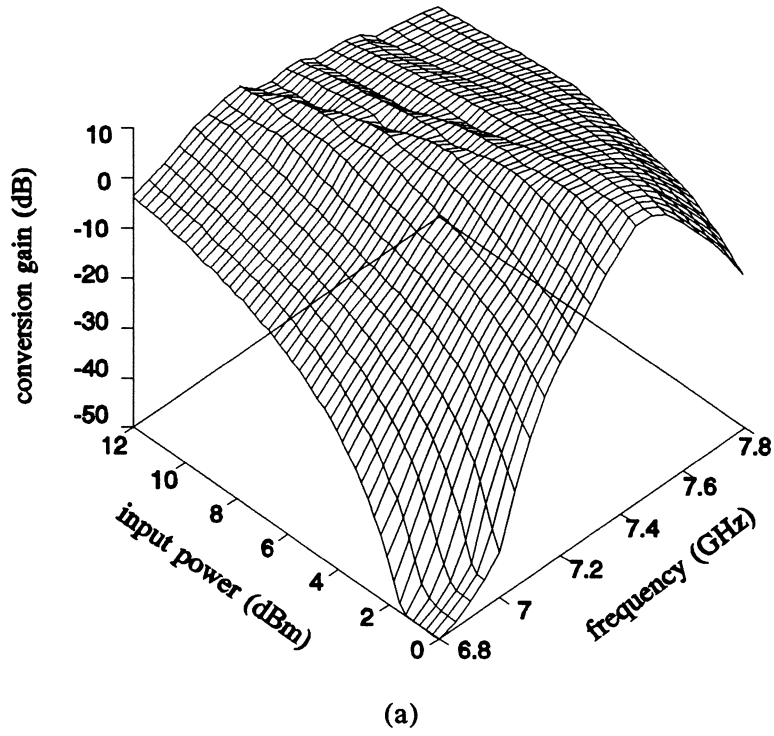


Fig. 10. 3D view of conversion gain versus input power and frequency, (a) before and (b) after optimization.

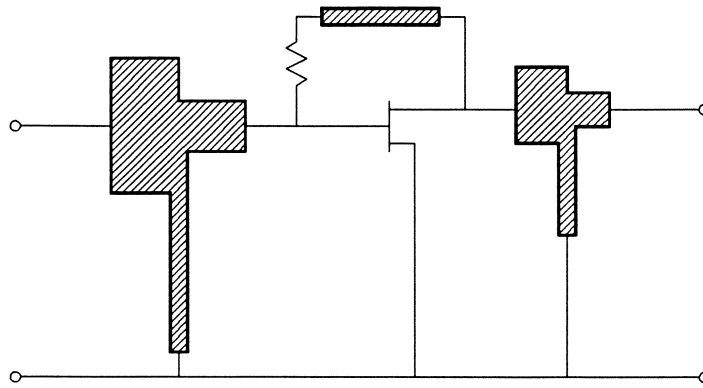


Fig. 11. Broad-band small-signal amplifier with microstrip components.

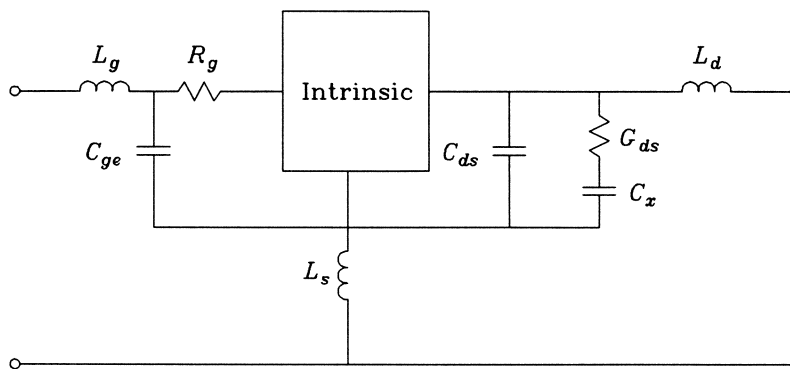


Fig. 12. Equivalent circuit for the SPICE MESFET model.

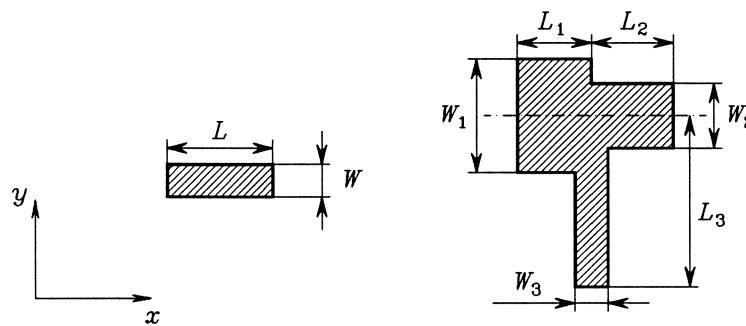


Fig. 13. Parameters of the feedback microstrip line and the microstrip T-structures.

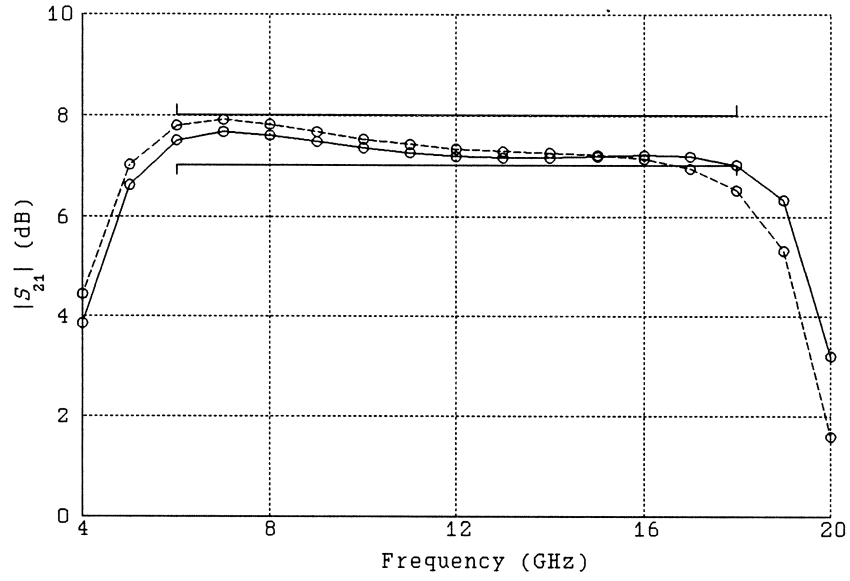
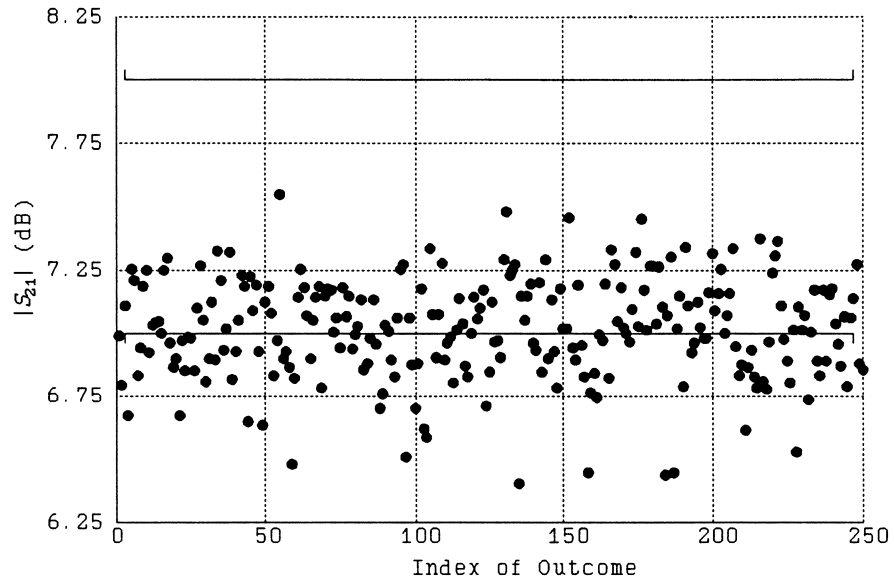
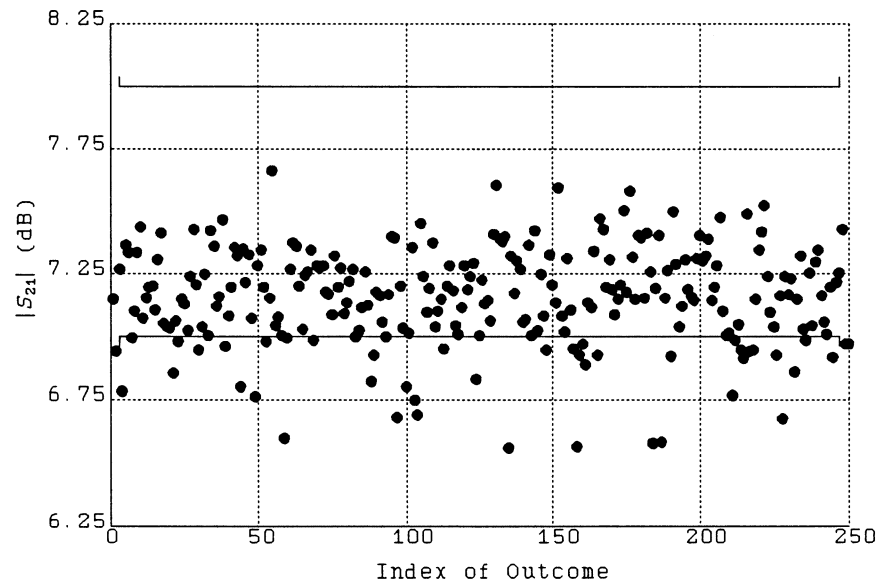


Fig. 14. $|S_{21}|$ response of the broad-band small-signal amplifier before (---) and after (—) nominal minimax design.



(a)



(b)

Fig. 15. Run charts of the $|S_{21}|$ response at 18 GHz (a) before and (b) after yield optimization. 250 outcomes are used.

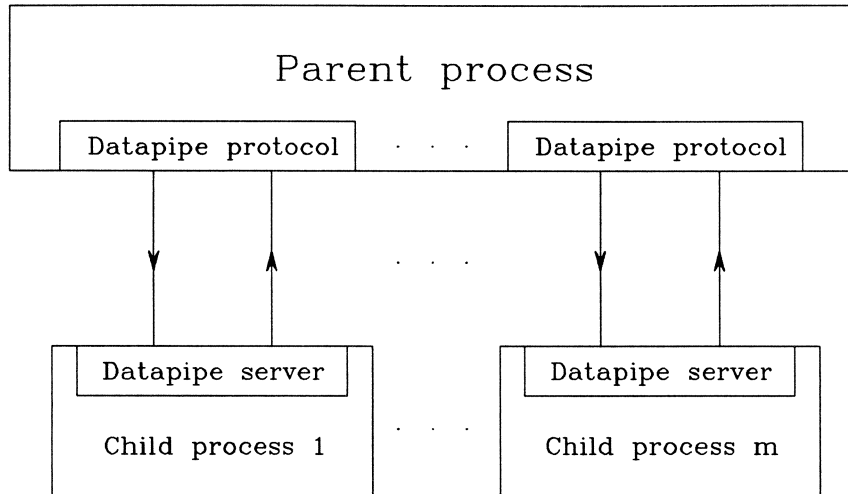


Fig. 16. Datapipe schematic.

